Applied Catalysis B: Environmental 220 (2018) 211–221

Contents lists available at ScienceDirect

Applied Catalysis B: Environmental

journal homepage: www.elsevier.com/locate/apcatb

Post treatment of composting leachate using ZnO nanoparticles immobilized on moving media

Alireza Ranjbari, Nader Mokhtarani*

Civil and Environmental Engineering Faculty, Tarbiat Modares University, 1411713116, Tehran, Iran

ARTICLE INFO

Keywords:
Leachate
Moving media
Nanoparticles
Photocatalyst
Toxicity
Zinc oxide

ABSTRACT

The capability of UV-ZnO photocatalytic process as a post treatment method for composting leachate was examined. ZnO nanoparticles immobilized on moving media were used for the first time in order to overcome the defects of photocatalytic processes such as the separation of nanoparticles in slurry systems as well as the need for more retention time in the conventional immobilized systems. The effect of factors such as pH, UV_C light intensity, concentration of immobilized nanoparticles, coated area and retention time was investigated. Based on the results of experiments, the maximum simultaneous COD and color removal of 61% and 71% were achieved respectively after 240 min of radiation with 32 W UV_C lamps in pH 11, in presence of 60 gr/m^2 immobilized ZnO and 400 cm^2 coated area. These values indicate 20% and 23% increase in COD and color removal compared with the maximum coatable surface on the reactor respectively. SPE-GC–MS analysis also revealed that the composting leachate contained various groups of organic compounds; most of which could be degraded into lower molecular weights, using photocatalytic process. In this research, the biodegradability of the leachate was also improved from 0.15 to 0.55 and the toxicity reduced by more than 79%.

1. Introduction

Industrial and economic development over recent decades in most countries along with changes in lifestyle has resulted in considerable growth of industrial and household waste. The amount of municipal solid waste (MSW) production in urban areas of Asia was approximately 0.76 million ton per day in 1998. Annual growth rate in developing countries and developed ones has also been reported as 2–3% and 3.2–4.5%, respectively [1]. In 1994, global MSW generation levels was approximately 1.3 billion tons/year (equivalent to 0.67 kg per capita per day), while it has amounted to 1.7 billion tons/year in 2004, indicating an increase of 31% [2]. MSW generation levels are expected to increase to approximately 2.2 billion tonnes per year by 2025 [3].

Leachate, a liquid manifestation from solid waste, has been considered as a serious environmental pollutant affecting natural resources as surface and ground waters, human health and hygiene [4]. Since biodegradable organic materials constitute approximately 60% of the total urban solid waste in developing countries, leachate treatment is considered as a big concern for waste management in these areas.

Common leachate treatment methods are classified into three groups: 1) leachate transmission method (recycling to landfill site and transmission to wastewater collection system and its treatment with urban wastewater); 2) biodegradation techniques including aerobic and anaerobic processes and 3) physiochemical treatment methods, such as chemical oxidation, absorption, chemical precipitation, flocculation and coagulation, floatation and precipitation, and advanced oxidation processes [5].

One common method in treatment of leachate is application of biological processes. However, due to significant organic load of leachate and presence of refractory pollutants, biological process alone cannot treat leachate on its own. In order to enhance the quality of leachate to the discharge standards, post treatment of biologically treated leachate is required [6,7].

One appropriate solution for complementary treatment of leachate and removal of refractory materials is the application of photo-catalytic processes. Use of photo-catalytic methods has attracted great deal of attention thanks to its unique features including full decomposition of contaminant to water and carbon dioxide, simple implementation, reusable materials, and quick removal of pollutants [8].

These processes, in which chemical pollutants are changed into inorganic materials, are based on production of hydroxyl radicals with high oxidation potency and the highest efficiency for oxidation of non-biodegradable compounds. The constituent molecules of photocatalyst such as TiO_2 and ZnO have semi-conductive properties. When the energy of an absorbed photon is equal to or more than the band gap which is about 3.09 eV (for ZnO), the electron is promoted from capacity band

* Corresponding author.
E-mail address: mokhtarani@modares.ac.ir (N. Mokhtarani).

http://dx.doi.org/10.1016/j.apcatb.2017.08.042
Received 29 May 2017; Received in revised form 26 July 2017; Accepted 14 August 2017
Available online 18 August 2017
0926-3373/

to conduction band, which causes generation of holes in the capacity band in response to electron stimulation [9]. Stimulated electrons and holes can produce hydroxyl radicals. These free radicals change organic materials into inorganic ones [10].

In photocatalytic treatment of leachate using slurry TiO_2 nanoparticles, maximum COD, BOD and TOC removal of 59%, 75%, and 80% was achieved respectively [11]. In another study, complementary treatment of landfill leachate (8 years old) was examined by photocatalytic UV-TiO_2 process. Based on the results, initial pH of the solution, nanoparticles concentration, and reaction time were reported as influential factors in the process. In this research, maximum COD removal of 60% and color removal of 97% were attained. BOD_5 to COD ratio of the solution was also enhanced from 0.09 to 0.39 implying increased leachate biodegradability [12].

In photocatalytic processes, two different methods including slurry and immobilized are usually used. In the slurry method, nanoparticles are dispersed in the solution, where the necessity to separate nanoparticles at the end of reaction and lack of reusability are the main disadvantage of this technique. Accordingly, various researches have tried to immobilize nanoparticles on different surface such as glass, quartz, silica, activated carbon, zeolite, etc. [13]. Immobilization method has also its own drawbacks, that the main one is reduction of active surface of nanoparticles.

In removal of Acid Red 27 using ZnO nanoparticles immobilized on glass, 90% removal of COD was obtained after 72 min [14]. The photocatalytic discoloration and degradation of C.I. Reactive Red 120 dye have been studied over ZnO nanoparticles immobilized on glass under sunlight. It was observed that complete dye decolorization and 90% of dye degradation was obtained after 60 and 180 min, respectively [15]. In another study, 95% removal of methyl orange by ZnO nanoparticles immobilized on glass surface was reported [16]. The photocatalytic efficiency of TiO_2 immobilized on various supports was compared with the photocatalytic efficiency of TiO_2 in suspension (2 g/L), for the degradation of 3-nitrobenzenesulfonic acid (3-NBSA) and 4-nitrotoluenesulfonic acid (4-NTSA). Based on the results, fixation of TiO_2 on solid supports appreciably reduces the photocatalytic efficiency [13]. Similarly, 95% removal of phenol from wastewater during photocatalytic process via immobilized TiO_2 nanoparticles on the concrete was reported [17]. Additionally, 88% removal of Hexavalent Chromium using ZnO nanoparticles stabilized on Kaolin was also reported by Shirzad et al. [18]. During photocatalytic post-treatment of composting leachate using TiO_2 nanoparticles immobilized on concrete surface, maximum simultaneous COD and color removal efficiency of 58% and 36% was reported respectively [7].

To utilize positive features of both slurry and immobilized methods, post treatment of composting leachate using ZnO nanoparticles coated on moving media through a photocatalytic process was selected as the main objective of this research. The effect of pH, concentration of immobilized nanoparticles, power of UV lamps, and area of moving media was examined. Degradation of different types of organic compounds during photocatalysis was also studied using gas chromatography coupled with mass spectrometry (GC/MS) analysis. It is believed that application of moving media coated with nanoparticles in photocatalytic process, has been used in this research for the first time and to the knowledge of the authors, no report has been published in this regard.

2. Materials and methods

2.1. Experimental system

This study was conducted in laboratory scale and batch mode. Schematic sketch of the system is illustrated in Fig. 1. The system consists of a Plexiglas column with 110 mm inner diameter, 300 mm height and total useful volume of 1000 mL. Philips UV_C lamps with different power levels ranging from 8 to 40 W were the sources of irradiation placed inside a quartz tube and mounted at the axial center of the reactor. In order to provide the necessary mixing, air was continuously injected into the column through a diffuser at the bottom of the reactor.

In each test, a certain amount of moving media coated with the nanoparticles were initially transferred into the reactor. Then the reactor was filled to a specified volume with the leachate. Finally, the reactions were started under a specified amount of UV_C radiation and at ambient temperature. Samples were collected at appropriate time intervals for analysis. Prior to analysis, the samples were centrifuged at 3000 rpm for 10 min and passed through a filter paper to remove all suspended particles. To prevent reflection and scattering of UV_C radiation in the environment, the reactor was covered with a thick layer of aluminum foil.

2.2. Preparation of moving media

Crystalline polypropylene plates (2 mm thickness) coated with different dosage of ZnO nanoparticles, having the density of about 1.07 g/cm^3 were used as moving media. To prepare the moving media, initially, both sides of the plates were coated with specified amount of ZnO nanoparticles and were cut to rectangular pieces with the dimension of 1.6*1.8 cm. They were connected two-by-two by creating a groove in the middle. Due to low melting point of polypropylene, it was not possible to use methods such as sol-gel requiring a high temperature for calcinations of nanoparticles. As a result, epoxy sealer method (ESM) was used to immobilize nanoparticles [17].

For this propose, thin layer of Metallplast glue (Razi Co., Iran) was dragged onto the media surface by a brush and maintained at laboratory temperature for 24 h to dry completely. Then, the surface was covered homogenously with a layer of glue (BAND-B202). After sonication of 20 g/L of ZnO suspension for 15 min in the ultrasonic bath, a desired amount of it was poured onto the glue surface to cover the entire surface. The ZnO coated surface was then exposed for 24–48 h at room temperature to dry out completely. Finally the coated surface was washed with distilled water to separate any mobilizes ZnO particles before being used as moving media inside the reactor.

2.3. Materials

Biological pre-treated leachate samples were collected from the effluent of leachate treatment facility of Gorgan composting plant in north of Iran. The characteristics of the effluent of this plant are summarized in Table 1.

In this plant, the organic load of leachate is significantly reduced through various biological and physical processes. However, according to Iranian Department of Environment (DOE), additional treatment is required to meet discharge standards [19]. This leads to the conclusion that a post treatment process for the effluent is mandatory.

Zinc oxide nanoparticles with an average particle size of 10–30 nm and with purity over 99% was supplied by US Research nanomaterial, Inc., USA. Commercial grade of sodium hydroxide and sulfuric acid were used for pH adjustment. All other chemicals employed for analysis were analytical grade and obtained from Merck Company.

2.4. Toxicity estimation

Washington university laboratory safety method was used to determine toxicity of the leachate [20,21]. For this purpose, based upon fish LC_{50} constituents of the leachate are divided into five categories as listed in Table 2. Then the equivalent toxicity of the leachate was calculated using Eq. (1).

$$\text{Toxicity}(\%) = \sum \text{X}\% + \frac{\sum \text{A}\%}{10} + \frac{\sum \text{B}\%}{100} + \frac{\sum \text{C}\%}{1000} + \frac{\sum \text{D}\%}{10000} \quad (1)$$

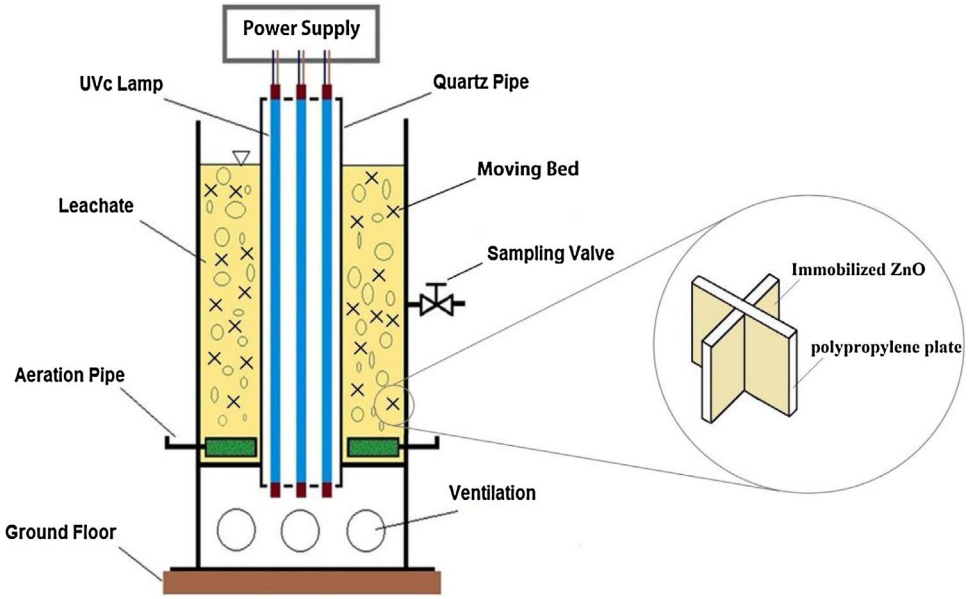

Fig. 1. Schematic of used batch photo-reactor.

Table 1
Leachate Characteristics.

Parameters	Concentration	Unit
COD	800	(mg/L)
BOD_5	125	(mg/L)
BOD_5/COD	0.15	–
TS	8000	(mg/L)
TSS	200	(mg/L)
EC	13	(μS/cm)
pH	9	–
Color	7	Gardner
Turbidity	80	(NTU)
Alkalinity	605	(mg/L as $CaCO_3$)

Table 2
Chemical Waste Toxicity Categories [22].

Toxic Category	Fish LC_{50} (ppm)
X	< 0.01
A	0.01– < 0.1
B	0.1– < 1.0
C	1.0– < 10.0
D	10.0–100.0

Where X, A, B, C and D are percentage of the leachate constituents associated with each toxicity categories. LC_{50} of each constituent of the leachate were also calculated using 4.2.1 TEST (Toxicity Estimation Software Tool) software [23].

2.5. Analytical procedures

Metrohm 691 pH meter with glass combination electrode was applied to measure pH. To ensure the absence of any suspended particles in samples, Sigma 101 centrifuge was used followed by MN 2 μm filter paper. Color and COD measurements were assayed at 780 nm and 640 nm, respectively, using a DR 4000 Hach spectrophotometer (Method 10105 and 8000).

Lutron RS-232 UV meter was utilized to measure the intensity of UV lamps radiation. Scanning electron microscope (SEM) −MIRA 3-equipped with EDX (Energy dispersive X-Ray) analysis system (TESCAN Co.) was used to investigate the quality of nanoparticles immobilized on media. A gas chromatograph (GC-7890A Agilent), coupled with a mass spectrometer (MS-5975C Agilent) was employed to determine the composition of intermediate products. The GC–MS applied for this purpose was equipped with a capillary column (Chrompak CP-Sil 8 CB, 50 m length, 250 μm internal diameter, 0.12 μm film thickness) and a liquid & headspace analyzer. The initial temperature of the column was set at 60 °C for 2 min. Increasing to 200 °C afterwards at a rate of 15 °C/min, immediately followed by further increase to 280 °C at a rate of 5 °C/min. One micro liter of split sample was injected into the GC column (with a split ratio of 1:5). All other parameters were analyzed according to the standard methods for the examination of water and wastewater [24].

3. Results and discussion

3.1. SEM analysis

SEM image of polypropylene substrate before and after immobilization of nanoparticles are depicted in Fig. 2. To investigate the nature of the coated nanoparticles, EDX analysis was performed whose results are presented in Fig. 3. As can be observed, a uniform layer of ZnO nanoparticles has been immobilized on the polymer substrate.

3.2. Reference experiments

Through a photocatalytic reaction, factors such as oxidant, photocatalyst, and energy source (UV_C light) help the reaction to proceed further. To prove effectiveness of all factors in a photocatalytic process, first the impact of every parameter on system was investigated both independently and in combination but without the concurrent presence of all factors.

Fig. 4 shows that the presence of photocatalyst (ZnO nanoparticles coated on moving media) with surface density of 60 g/m^2 (lack of UV_C light) has no significant effect on the organic load removal of leachate on its own and only 1% of solution COD is removed after 120 min. It can be attributed to the lack of stimulation in nanoparticles due to absence of UV_C light and thus no generation of hydroxyl radicals.

In aeration processes alone and concurrent application of aeration and photocatalyst, maximum COD removal of 3.5% and 4.4%, were obtained respectively. UV_C light alone brought about an 8% removal, while maximum COD removal efficiency of 12.5% was obtained when UV_C and aeration were utilized simultaneously.

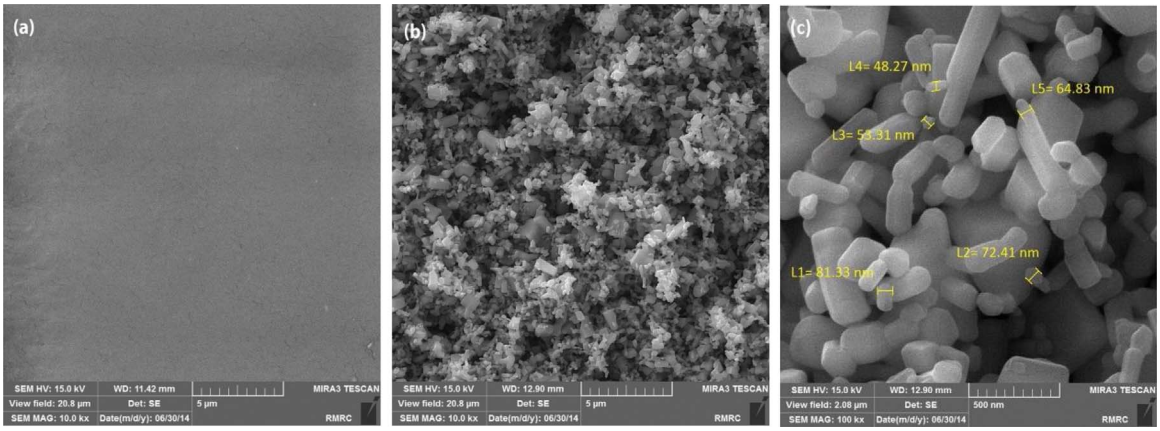

Fig. 2. SEM images of moving media.
(a) before coating (b) after coating (c) dimensions of immobilized ZnO

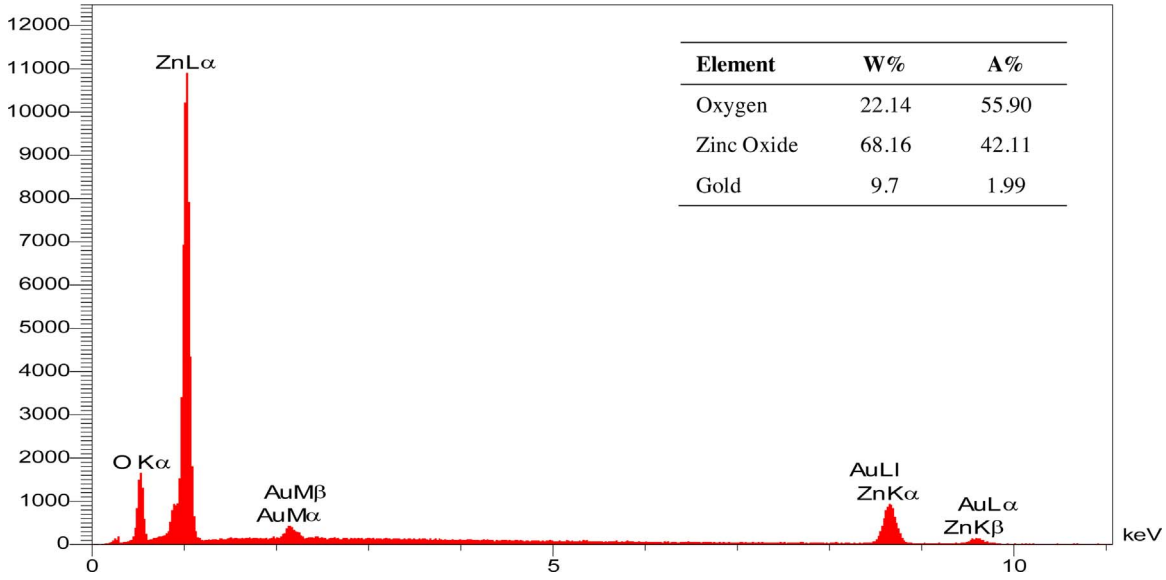

Element	W%	A%
Oxygen	22.14	55.90
Zinc Oxide	68.16	42.11
Gold	9.7	1.99

Fig. 3. EDX analysis of immobilized nanoparticles on moving media.

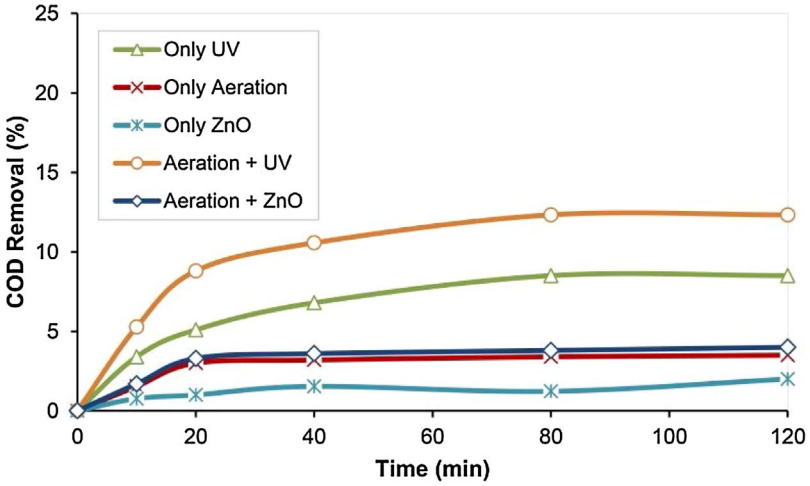

Fig. 4. Control experiments.
(pH = 9, UV = 40 W, ZnO = 60 gr/m^2, Aeration = 2 L/min)

3.3. The effect of pH

pH is one of the effective parameters in photocatalytic process. The initial pH value can affect various factors including: surface charge, oxidation and reduction potential, and position of energy bands of nanoparticles [25]. Fig. 5 represents leachate COD removal at various pH using ZnO with an immobilized nanoparticles concentration of 60 g/m^2 (400Cm^2 coated area) and UV$_C$ lamps power adjusted to 32W. As shown by increasing pH, the COD removal efficiencies were also increased and after 180 min reached its maximum value (62%) at pH

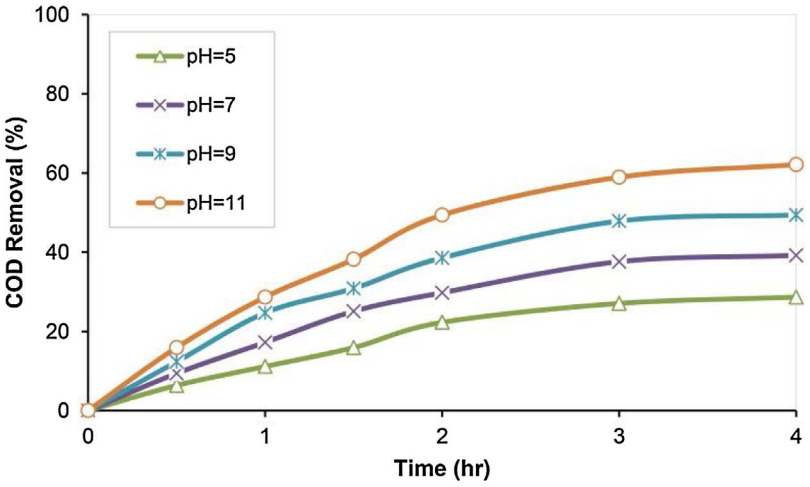

Fig. 5. Effect of pH on COD removal.
(ZnO = 60 gr/m^2, Coated Surface = 400 cm^2, UV = 32 W)

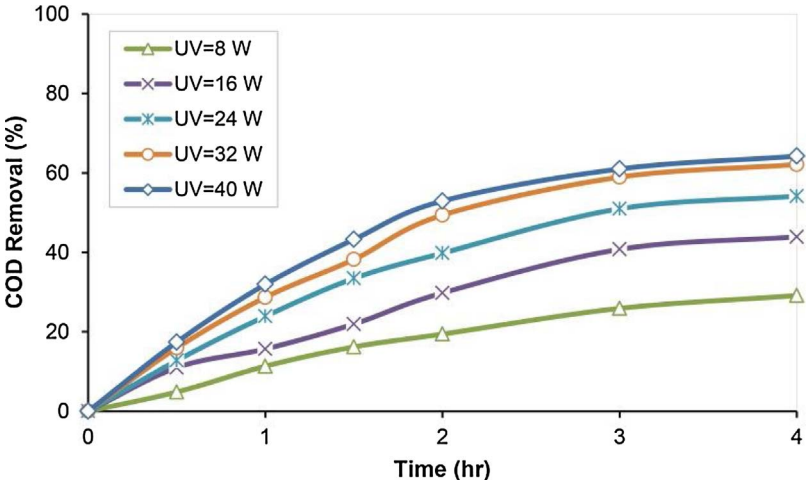

Fig. 6. Effect of UVc lamps power on COD removal.
(pH = 11, Coated Surface = 400 cm^2, ZnO = 60 gr/m^2)

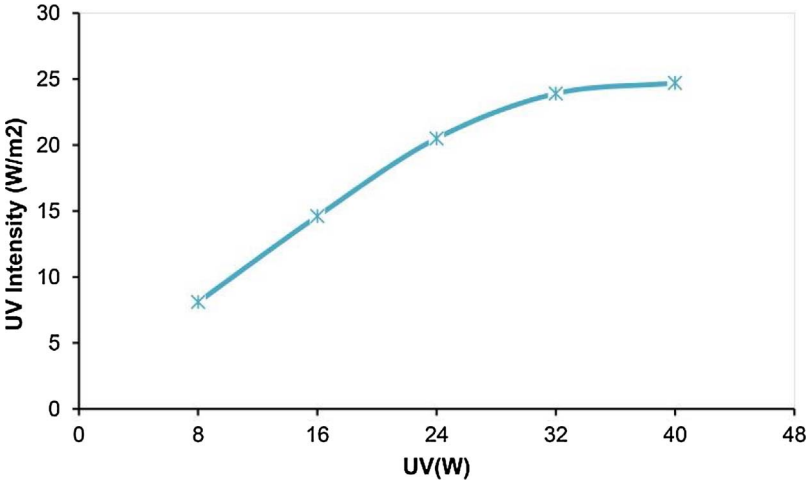

Fig. 7. Relation between power and light intensity of UVc lamps inside the reactor.

11.

The increase in removal efficiency at alkaline conditions can be related to the ability of photocatalytic process to initiate hydroxyl radical formation at high pH. Eqs. (2)–(7) indicate that hydroxide ions can be directly stimulated through the photocatalytic reactions and change into hydroxyl radicals [26]. Due to its high oxidation and reduction potential, hydroxyl radical plays an important role in the degradation of organic compounds.

$$ZnO + hv\ (UV) \rightarrow ZnO\ (e^- CB + h^+ VB) \quad (2)$$

$$ZnO\ (e^- CB) + ZnO\ (h^+ VB) \rightarrow Heat \quad (3)$$

$$ZnO\ (h^+ VB) + H_2O \rightarrow ZnO + H^+ + OH\cdot \quad (4)$$

$$ZnO\ (h^+ VB) + OH^- \rightarrow ZnO + OH\cdot \quad (5)$$

$$Organic\ Materials + OH\cdot \rightarrow Intermediates \quad (6)$$

$$Intermediates + OH\cdot \rightarrow Final\ Products \quad (7)$$

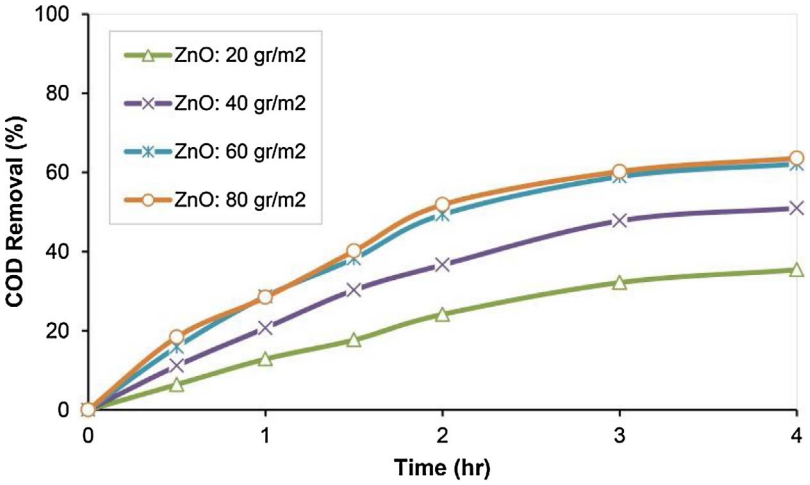

Fig. 8. Effect of immobilized nanoparticles concentration on COD removal.
(pH = 11, Coated Surface = 400 cm^2, UV = 32 W)

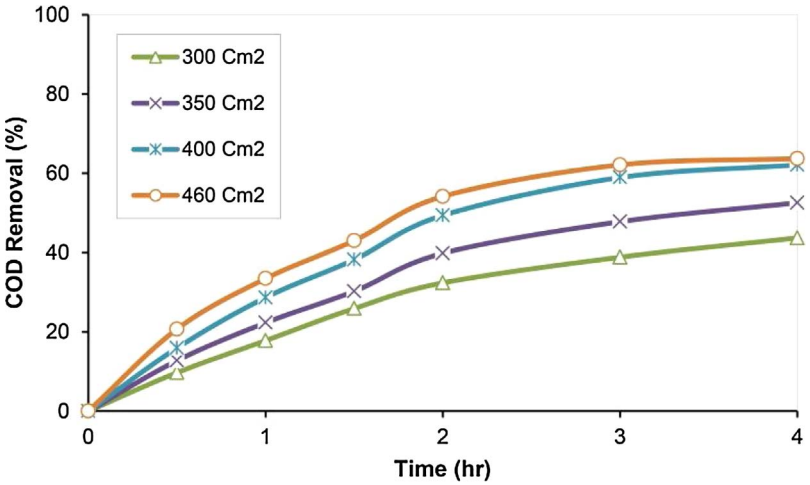

Fig. 9. Effect of moving media coated area on COD removal.
(pH = 11, UV = 32w, ZnO = 60 gr/m^2)

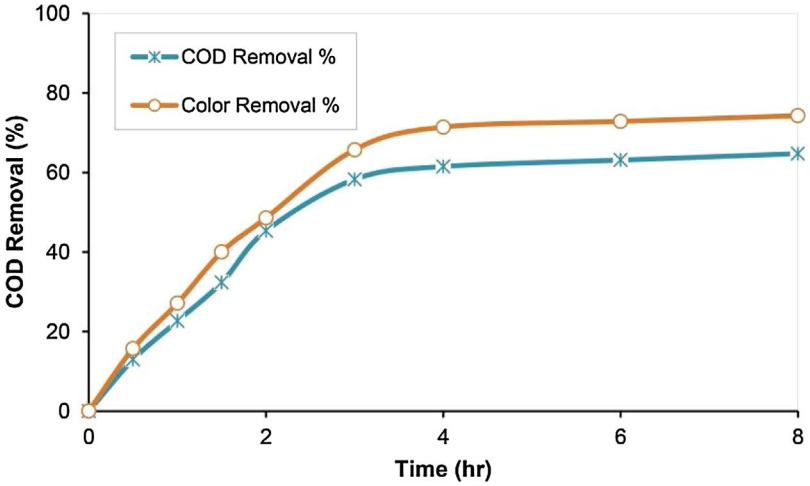

Fig. 10. Effect of irradiation time on the COD and color removal efficiency.
(UV = 32 W, pH = 11, Coated Surface = 400 cm^2, ZnO = 60 gr/m^2)

Since higher pH levels are difficult to use in full-scale, pH value greater than 11 were not examined in this study. Due to photo-decomposition of ZnO nanopowder in acidic solutions the effect of pH lower than 5 was also disregarded in this research [27]. In a similar study, the removal efficiency of 2-Chlorophenol using UV-ZnO photocatalytic process was also found to increase with increasing the pH. [28].

3.4. Light intensity

To investigate the effect of light intensity, experiments were repeated by several UV_C lamps; the results are presented in Fig. 6.

As can be seen, by increasing the lamps power, the removal rate was also increased. However, there is no linear relationship between these two parameters. Here by increasing the lamp power from 8 to 16 W, COD removal efficiency grew about 15%, but this development reached only 2% when the power was further increased from 32 to 40 W. In a

Table 3
Removal efficiency of slurry and immobilized moving bed system.

Irradiation Time (hr)	COD Removal (%)		Color Removal (%)	
	Slurry	Immobilized	Slurry	Immobilized
1	31	23	36	27
2	54	45	62	49
3	57	58	67	66
4	58	62	70	71
6	60	63	71	73
8	62	65	72	74

similar study, COD removal efficiency of 70%, 90%, and 98% were obtained using 16, 32, and 64W UV_C lamps respectively, for the removal of terephthalic acid through a UV-ZnO photocatalytic process [25].

As the power of lamp and thus intensity of radiation increases, the particulates of photocatalytic materials are further stimulated and thereby producing further hydroxyl radicals culminating in enhanced COD removal. However, because of the reactor shape and low distance between UV_C sources and surface of media, further increasing of UV_C lamps power would not lead to increased radiation intensity inside the reactor [29]. As a result, according to Fig. 7 the intensity of radiation inside the reactor reached its maximum after some time and further increase of lamps power cannot promote it significantly.

3.5. Immobilized nanoparticles concentration

In order to examine the effect of immobilized nanoparticles

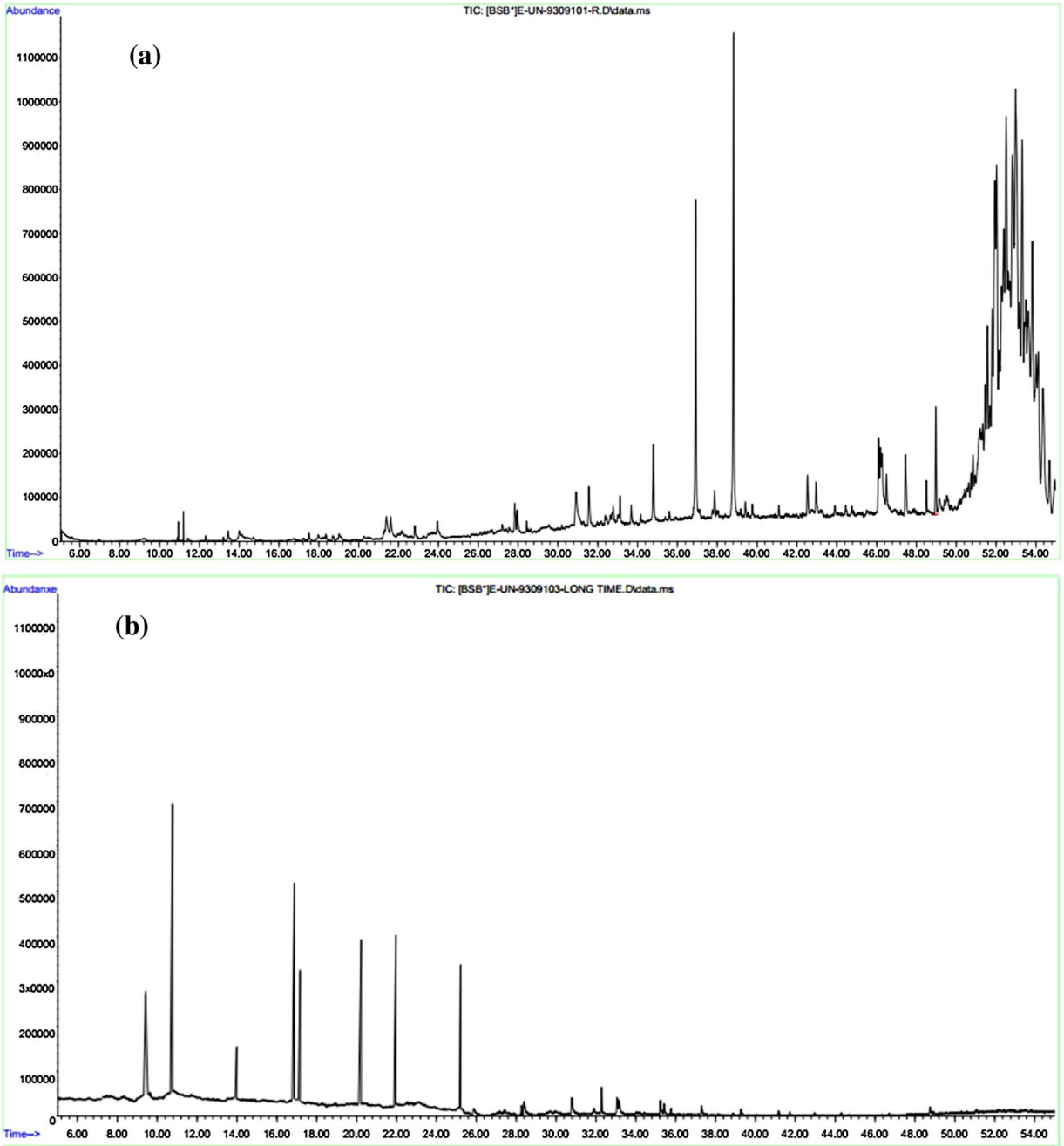

Fig. 11. GC-Mass spectrum of leachate.
(a) Before photocatalytic treatment (b) After photocatalytic treatment

Table 4
Leachate identified constituents (before process).

Peak No.	Compound	Retention Time (min)	Fish LC_{50} (ppm)	Area%
1	Perhydro-htx-2-one, 2-depentyl-, acetate ester	13.997	9.8	0.17
2	Methenamine	21.390	6646.48	0.37
3	Benzene, 1-phenyl-4-(2-cyano-2-phenylethenyl)	21.607	2.92E-02	0.26
4	1H-Indole, 1,3-dimethyl-5,6-dimethoxy-2-(3,5-dimethoxyphenyl)-	23.954	1.24	0.22
5	Decane, 1-chloro-	27.836	0.51	0.31
6	Cyclopentane, (2-methylpropyl)-	27.968	2.39	0.25
7	1H-Inden-1-one, octahydro-7a-methyl-, trans-	30.913	62.58	0.72
8	Phenol, 4-(1,1,3,3-tetramethylbutyl)-	31.556	2.17	0.43
9	Cyclopentane, 1-pentyl-2-propyl-	32.772	0.65	0.16
10	Phenol, 2,4-di-t-butyl-6-nitro-	33.129	0.28	0.18
11	Oxalic acid, dodecyl isobutyl ester	33.687	2.57	0.16
12	Phenanthrene, 9,10-dihydro-	34.795	1.49	0.66
13	Phthalic acid, cyclohexyl isohexylester	36.918	0.63	2.75
14	Phthalic acid, isobutyl non-5-yn-3-yl ester	37.863	0.21	0.22
15	1,2-Benzenedicarboxylic acid, butyl octyl ester	38.824	1.21	4.04
16	Cyclotetradecane, 1,7,11-trimethyl-4-(1-methylethyl)-	39.421	0.56	0.13
17	2-Furancarboxylic acid, 4-chlorobenzyl ester	39.769	0.24	0.14
18	Ethanol, 2-[2-[4-(1,1,3,3-tetramethylbutyl)phenoxy]ethoxy]-	42.536	5.45	0.34
19	1,3-Diamino-8-methylbenzo[f]quinazoline	42.729	5.03	0.16
20	1,8-Diethyl-3,6-diazahomoadamantan-9-ol	42.954	143.64	0.37
21	5-Aminohexanoic acid	46.108	204.91	0.64
22	L-Valine, N-cyclopentylcarbonyl-,methyl ester	46.201	14.22	0.67
23	L-Valine, N-cyclopentylcarbonyl-,methyl ester	46.278	14.22	0.78
24	N-Acetyl-2-aminovaleric acid	46.495	169.16	0.38
25	Ethanol, 2-[2-[2-[4-(1,1,3,3-tetramethylbutyl)phenoxy]ethoxy]ethoxy]	47.448	8.29	0.61
26	Cyclotetrasiloxane, octamethyl-	48.510	0.022	0.22
27	Phthalic acid, 2-ethylhexyl isohexyl ester	48.975	1.95	0.72
28	Acrylophenone, 3,3-diphenyl-, semicarbazone	49.153	0.14	0.28
29	7a,9c-(Iminoethano)phenanthro[4,5-bcd]furan, 4a.alpha.,5-dihydro-3-methoxy-12-methyl-	49.409	0.48	0.13
30	Ethyl 2-methyl-3-oxocyclopentane-1-carboxylate	49.533	85.02	0.31
31	1,2-Benzenedicarboxylic acid, monobutyl ester	50.416	10.98	0.2
32	Phthalic acid, 5-methoxy-3-methylpent-2-yl nonyl ester	50.532	1.23	0.19
33	Phthalic acid, 2-(2-methoxyethyl)hexyl nonyl ester	50.625	0.72	0.26
34	1,2-Benzenedicarboxylic acid, diundecyl ester	50.741	7.69E-02	0.29
35	Phthalic acid, isohexyl isoporpylester	50.842	1.9	0.5
36	Phthalic acid, isobutyl 2-(2-methoxyethyl)hexyl ester	50.943	3.02	0.34
37	Phthalic acid, decyl 2-(2-methoxyethyl)hexyl ester	51.183	0.94	1.75
38	Phthalic acid, 2-(2-methoxyethyl)hexyl nonyl ester	51.261	0.72	0.5
39	Phthalic acid, bis(7-methyloctyl)ester	51.330	0.43	0.86
40	Phthalic acid, neopentyl octyl ester	51.462	0.6	1.5
41	Phthalic acid, neopentyl nonyl ester	51.563	0.3	2.11
42	Phthalic acid, cyclohexyl neopentyl ester	51.694	0.6	1.28
43	Phthalic acid, neopentyl nonyl ester	51.811	0.3	2.27
44	Phthalic acid, bis(7-methyloctyl)ester	51.942	0.43	4.41
45	Phthalic acid, 1-cyclopentylethyl nonyl ester	52.028	0.62	4.09
46	Phthalic acid, 2-(2-methoxyethyl)hexyl nonyl ester	52.152	0.72	1.88
47	Phthalic acid, nonyl 2-pentyl ester	52.276	0.93	2.75
48	Phthalic acid, nonyl 4-octyl ester	52.384	0.28	4.02
49	Phthalic acid, bis(7-methyloctyl)ester	52.508	0.43	5.73
50	Phthalic acid, nonyl 4-octyl ester	52.609	0.28	2.32
51	Phthalic acid, 1-cyclopentylethyl nonyl ester	52.679	0.62	2.18
52	Phthalic acid, decyl 2-isopropoxyphenyl ester	52.826	0.28	6.32
53	Phthalic acid, isobutyl pentadecylester	52.981	4.76E-02	9.04
54	1,2-Benzenedicarboxylic acid, dinonyl ester	53.151	0.11	2.72
55	1,2-Benzenedicarboxylic acid, isodecyl octyl ester	53.314	0.36	4.79
56	Phthalic acid, 2-cyclohexylethyl nonyl ester	53.446	0.13	1.87
57	Phthalic acid, (2-chlorocyclohexyl)methyl nonyl ester	53.500	0.45	1.64
58	1,2-Benzenedicarboxylic acid, dinonyl ester	53.616	0.11	3.95
59	Phthalic acid, dodecyl nonyl ester	53.825	7.92E-02	4.31
60	1,2-Benzenedicarboxylic acid, decyl hexyl ester	54.019	0.34	2.01
61	Phthalic acid, 2-acethylphenyl nonyl ester	54.128	0.21	1.78
62	Phthalic acid, hexyl tetradecyl ester	54.345	0.12	2.29
63	1,2-Benzenedicarboxylic acid, dinonyl ester	54.685	0.11	0.64
64	Phthalic acid, nonyl pentadecyl ester	54.941	1.30E-02	0.35

concentration on the COD removal efficiency experiments were repeated with 20, 40, 60, and 80 g/m^2 catalyst coated on the moving media. As shown in Fig. 8, when the surface density of photocatalyst increased from 20 to 60 g/m^2, COD removal rose from 35 to 62%. However, when it was further increases up to 80 g/m^2, removal efficiency did not experience any significant increase and reached 64%, signifying an only 2% growth.

As the amount of photocatalyst initially increases, the amount of hydroxyl radical production, and in turn COD removal yield increase. Nevertheless, further addition of photocatalyst material would result in aggregation of ZnO on the media due to constancy of the surface and its saturation, implying no further yield development. Similar results have also been reported when composting leachate was treated with TiO_2 nanoparticles immobilized on concrete surface [7].

Table 5
Leachate identified constituents (after process).

Peak No.	Compound	Retention Time (min)	Fish LC_{50} (ppm)	Area%
1	2-Pentanone, 4-hydroxy-4-methyl-	10.729	2283.51	21.36
2	Benzene, 1,2,3-trimethyl-	14.052	11.84	5.13
3	1-Tridecene	15.155	0.15	0.08
4	2,6-Dimethyl-1,3,5,7-octatetraene,E,E	15.984	0.82	0.09
5	Undecane	16.953	0.4	9
6	Benzo[h]quinoline, 2,4-dimethyl-	17.228	0.88	5 .12
7	2,6-Dimethyldecane	18.928	0.51	0.04
8	Dodecane	20.251	0.24	10.12
9	Dodecane, 4,6-dimethyl-	21.329	0.29	0.04
10	1,2-Benzenediol, 3,5-bis (1,1-dimethylethyl)-	21.543	1.67	0.05
11	Tridecane	22.097	0.15	9
12	Tetradecane	25.573	0.13	9 .13
13	Hexatriacontane	27.364	0.019	0.09
14	Pentadecane	28.309	0.12	0.25
15	Hexadecane	30.704	0.14	0.14
16	Hexadecane, 2,6,11,15-tetramethyl-	31.826	0.52	0.06
17	Eicosane, 2-methyl-	32.344	0.19	0.05
18	Hexadecane, 2,6,10,14-tetramethyl-	33.112	0.16	0.06
19	Octadecane	35.136	0.2	0.1
20	Nonadecane	37.19	0.14	0.09
21	Eicosane	39.152	0.086	0.06
22	Heptadecane, 2,6,10,15-tetramethyl	41.024	0.22	0.06
23	Heptadecane	44.541	0.12	0.04
24	Phthalic acid, isohexyl isoporpylester	45.229	1.9	0.05
25	Phthalic acid, 2-ethylhexyl isohexyl ester	48.594	1.95	0.04

3.6. Moving media surface area

Surface area of moving media coated with nanoparticles is another effective parameter in this process. If the number of moving media and thus area coated with nanoparticles is not sufficient, the active sites provided by the presence of ZnO are low in number; resulting in reduced removal efficiency. Similarly, if their numbers inside the reactor are more than necessary, the removal again declines in response to convolution of the media and insufficient UV_C exposure.

In this experiment, the minimum area of media was selected to be 300 cm^2 (equal to lateral area of outer reactor wall). Fig. 9 depicts that COD removal efficiency reached 42%, 53%, 62%, and 64% after 4 h, through the application of moving media with useful surface areas of 300, 350, 400, and 460 cm^2, respectively.

As shown by increasing the number of media, and in turn the surface coated with nanoparticles (increasing of active sites), COD removal efficiency is enhanced. However, when the number of media increases further, due to convolution of nanoparticles and limitation in receiving UV_C radiation the system removal efficiency does not change significantly. Here by increasing the surface area from 300 cm^2 to 400 cm^2, COD removal efficiency grew about 20%, but this development was insignificant (less than 2%) when the surface area was further increased from 400 cm^2 to 460 cm^2. Therefore, 400 cm^2 media surface area (approximately 32% more than the reactor outer wall area), was chosen as the basis for subsequent experiments.

3.7. Irradiation time

In order to investigate the effect of irradiation time, some experiments were carried out with 32 W UV_C lamps (2.5 mW/Cm^2 light intensity), pH = 11, ZnO surface density of 60 g/m^2 and in the presence of 400 cm^2 surface area of moving media (Fig. 10).

Similarly, COD removal and color removal accomplished within the first 4 h of reaction were faster than the second four hours. Regarding the considerably short lifespan of hydroxyl radicals (only a few nanoseconds), they can only cause oxidation at the formation site or somewhere very close to that [30]. Since in a photocatalytic process, the major oxidation factor is hydroxyl radicals [31]; therefore, at the onset of reaction, the rate of reaction progression is higher due to the presence of more pollutants at the site of hydroxyl radical formation. With regard to the results obtained, the optimal retention time for photocatalytic treatment of leachate was taken to be 4 h, where 62% and 71% removal efficiency were obtained for COD and color, respectively.

As it is known, ZnO undergoes photo-corrosion under UV irradiation, which results decrease in photocatalytic activity [32,33]. In order to examine the stability of nanoparticles immobilized on the media, COD removal efficiency was measured after 20 times of frequent usage. The results revealed that reduction in removal efficiency was lower than 2% which represents a relatively low photo-corrosion (data not shown in this paper).

Although there are several ways to enhance photocatalytic ability of immobilized zinc oxide (such as: modification in shape, size and surface properties of ZnO, increase wavelength response range, and dope metals, non-metals and rare earth elements in host lattice) but they were not within the framework of this research. [34–37].

In order to compare the removal efficiency of immobilized process with those of slurry system, experiments were repeated with 1 gr/L of ZnO nanoparticles suspension (instead of moving media) under the same conditions [38]. The results of color and COD removal efficiency for both systems are summarized in Table 3. As shown after 4 h irradiation the maximum removal efficiency was approximately achieved

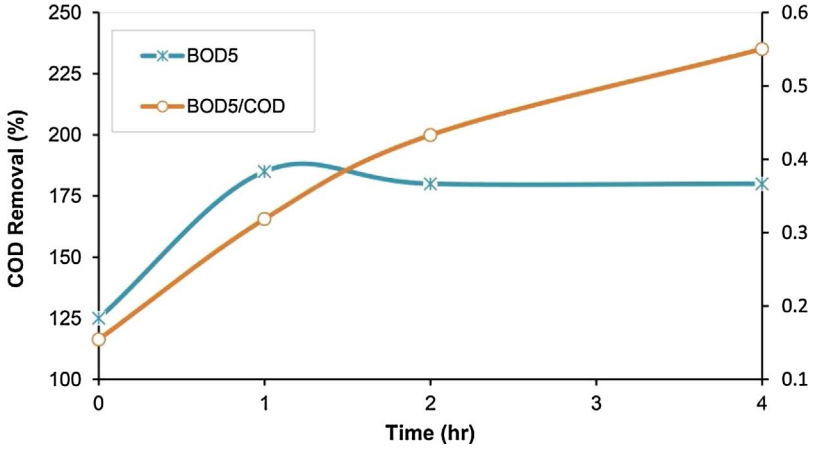

Fig. 12. BOD_5 and BOD_5/COD changes during photo-catalytic process.

for both processes and after those the changes in COD and color removal were insignificant. Therefore, by using nanoparticles immobilized on the moving media besides achieving the same removal as slurry process, difficulties of separation of suspended nanoparticles from wastewater has also been resolved.

As can be seen in Table 3 in irradiation time of less than 3 h the removal efficiency of slurry process were almost greater than immobilized system; which can be attributed to a decrease in the effective surface area of the immobilized photocatalyst compared with the nanoparticles in suspension [13].

3.8. Degradation of contaminant during the process

One salient feature of leachate is the existence of refractory compounds in it. In a photocatalytic process, hydroxyl radicals react with heavy and cyclic molecules available in solution and convert them into simpler and smaller molecules that can enhance biodegradability; thereby BOD of the solution [39].

In this research, GC-Mass analysis was used to determine intermediate reaction products. The SPE-GC-Mass spectrums of the leachate before and after photocatalytic processes are represented in Fig. 11. Table 4 and 5 list the main products identified in chromatograms using NIST library.

As can be seen peaks have emerged at longer retention times implying the existence of compounds heavier than the treated leachate before photocatalytic reaction. To ensure degradation of heavy compounds and to convert them to simpler molecules, the BOD_5 of leachate was measured. Fig. 12 shows that BOD_5 of the solution increased from about 125–185 mg/L after one hour from photocatalytic process, almost leveling off thereafter. Nevertheless, due to reduction in COD during the process, BOD_5/COD ratio has developed significantly to such an extent that it reached 0.55 at the end of treatment process from 0.15 at the process onset.

In this study toxicity of the leachate before and after photocatalytic process was also calculated to be 2.158% and 0.450% respectively, which imply a good toxicity reduction during this process.

4. Conclusion

For the first time, photocatalytic process was investigated using ZnO nanoparticles immobilized on moving media in the post treatment of composting leachate. In this study, the effect of pH, concentration of immobilized nanoparticles, power of UV_C lamps, irradiation time and media surface area were examined throughout the process. Based on the obtained results, the use of moving media instead of fixed bed for nanoparticles immobilization provided the possibility of increasing the coated area as well as effective contact between nanoparticles and the leachate; culminating in enhanced organic load and color removal efficiency. In this research, maximum organic load removal efficiency was obtained after 4 h irradiation with 32W UV_C lamps in pH = 11 and in the presence of 400 cm^2 of media surface area coated with 60 g/m^2 ZnO nanoparticles. Under these conditions, maximum COD and color removal efficiency were 61% and 71%, respectively; suggesting a 20% increase in removal compared to when using a 300 cm^2 of coated media (max coatable area of the reactor). GC-Mass analysis also indicated that existing organic compounds in the leachate change into simpler and less toxic compounds through photocatalytic processes, where BOD_5/COD ratio increased from 0.15 in raw leachate to 0.55 in treated leachate and the toxicity reduced by more than 79%. The results suggest that immobilized ZnO photocatalytic process with moving media is an effective chemical oxidation process on the post treatment of composting leachates.

Acknowledgements

This work was partially supported by the Iran Nanotechnology Initiative Council; and Tarbiat Modares University (TMU) research fund.

References

[1] A.M. Damghani, G. Savarypour, E. Zand, R. Deihimfard, Municipal solid waste management in Tehran: current practices, opportunities and challenges, Waste Manage. 28 (2008) 929–934.
[2] K.Y. Foo, B.H. Hameed, An overview of landfill leachate treatment via activated carbon adsorption process, J. Hazard. Mater. 171 (2009) 54–60.
[3] D. Hoornweg, P. Bhada-Tata, What a waste: a global review of solid waste management, Urban Development Series; Knowledge Papers No. 15, World Bank, Washington, DC, 2012.
[4] B.P. Naveen, D.M. Mahapatra, T.G. Sitharam, P.V. Sivapullaiah, T.V. Ramachandra, Physico-chemical and biological characterization of urban municipal landfill leachate, Environ. Pollut. 220 (2017) 1–12.
[5] J. Wiszniowski, D. Robert, J. Surmacz-Gorska, K. Miksch, J.V. Weber, Landfill leachate treatment methods: a review, Environ. Chem. Lett. 4 (2006) 51–61.
[6] I. Oller, S. Malato, J.A. Sánchez-Pérez, Combination of advanced oxidation processes and biological treatments for wastewater decontamination: a review, Sci. Total Environ. 409 (2011) 4141–4166.
[7] N. Mokhtarani, S. Khodabakhshi, B. Ayati, Optimization of photocatalytic post-treatment of composting leachate using UV/TiO_2, Desalin. Water Treat. 57 (2016) 22232–22243.
[8] S.S. Priya, M. Premalatha, N. Anantharaman, Solar photocatalytic treatment of phenolic wastewater potential, challenges and opportunities, J. Eng. Appl. Sci. 3 (2008) 36–41.
[9] N.K. Singh, S. Saha, A. Pal, Solar light-induced photocatalytic degradation of methyl red in an aqueous suspension of commercial ZnO: a green approach, Desalin. Water Treat. 53 (2015) 501–514.
[10] A. Akyol, M. Bayramoglu, Photocatalytic performance of ZnO coated tubular reactor, J. Hazard Mater 180 (2010) 466–473.
[11] S.P. Cho, S.C. Hong, S.I. Hong, Photocatalytic degradation of the landfill leachate containing refractory matters and nitrogen compounds, Appl. Catal. B-Environ. 39 (2002) 125–133.
[12] C. Jia, Y. Wang, C. Zhang, Q. Qin, UV-TiO_2 photocatalytic degradation of landfill leachate, Water Air Soil. Poll. 217 (2011) 375–385.
[13] A. Rachel, M. Subrahmanyam, P. Boule, Comparison of photocatalytic efficiencies of TiO_2 in suspended and immobilized form for the photocatalytic degradation of nitrobenzenesulfonic acids, Appl. Catal. B-Environ. 37 (2002) 301–308.
[14] M.A. Behnajady, N. Modirshahla, N. Daneshvar, M. Rabbani, Photocatalytic degradation of CI Acid Red 27 by immobilized ZnO on glass plates in continuous-mode, J. Hazard. Mater. 140 (2007) 257–263.
[15] M.Y. Ghaly, M.E.M. Ali, L. Österlund, I.A. Khattab, M.I. Badawy, J.Y. Farah, F.M. Zaher, M.N. Al-Maghrabi, ZnO/spiral-shaped glass for solar photocatalytic oxidation of Reactive Red 120, Arab. J. Chem. 10 (2017) S3501–S3507.
[16]. H. Khalilian, M. Behpour, V. Atouf, S.N. Hosseini, Immobilization of S, N-codoped TiO_2 nanoparticles on glass beads for photocatalytic degradation of methyl orange by fixed bed photoreactor under visible and sunlight irradiation, Sol. Energy 112 (2015) 239–245.
[17] M. Delnavaz, B. Ayati, H. Ganjidoust, S. Sanjabi, Kinetics study of photocatalytic process for treatment of phenolic wastewater by TiO_2 Nano powder immobilized on concrete surfaces, Toxicol. Environ. Chem. 94 (2012) 1086–1098.
[18] M. Shirzad-Siboni, A. Khataee, B. Vahid, S.W. Joo, S. Fallah, Preparation of a green photocatalyst by immobilization of synthesized ZnO nanosheets on scallop shell for degradation of an azo dye, Curr. Nanosci. 10 (2014) 684–694.
[19] A.M. Shaeri, A. Rahmati, Human's Environmental Laws, Regulations, Criteria and Standards. Department of Environment (DOE), Hak publishing Co., Tehran, 2012.
[20] University of Washington, Laboratory safety manual, Section 3, chemical waste management, UW Environmental Health and Safety, 1–20. http://www.ehs.washington.edu/manuals/lsm/lsm3.pdf, 2015 (Accessed on 3.12.2016).
[21] A. Soubh, N. Mokhtarani, The post treatment of composting leachate with a combination of ozone and persulfate oxidation processes, RSC Adv. 6 (2016) 76113–76122.
[22] J.H. Sun, X.Y. Li, J.L. Feng, X.K. Tian, Oxone/Co^{2+} oxidation as an advanced oxidation process comparison with traditional Fenton oxidation for treatment of landfill leachate, Water Res. 43 (2009) 4363–4369.
[23] Toxicity Estimation Software Tool, https://www.epa.gov/chemical-research/toxicity-estimation-software-tool-test, 2016 (Accessed on 3.12.2016).
[24] APHA, Standard,Method for the Examination of Water and Wastewater, 21st ed., American Public Health Association, Washington, D.C., USA), 2005.
[25] A. Shafaei, M. Nikazar, M. Arami, Photocatalytic degradation of terephthalic acid using Titania and zinc oxide photocatalysis: comparative study, Desalination 252 (2010) 8–16.
[26] M.A. Behnajady, N. Modirshahla, R. Hamzavi, Kinetic study on photocatalytic degradation of CI Acid Yellow 23 by ZnO photocatalyst, J. Hazard. Mater. 133 (2006) 226–232.
[27] N. Daneshvar, M.H. Rasoulifard, A.R. Khataee, F. Hosseinzadeh, Removal of CI Acid Orange 7 from aqueous solution by UV irradiation in the presence of ZnO nanopowder, J. Hazard. Mater. 143 (2007) 95–101.
[28] M.A. Barakat, H. Schaeffer, G. Hayes, S. Ismat-Shah, Photocatalytic degradation of 2-chlorophenol by co-doped TiO_2 nanoparticles, Appl. Catal. B-Environ. 57 (2005) 23–30.
[29] S. Li, M. Zichuan, Z. Jie, W. Yinsu, G. Yamin, A comparative study of photocatalytic

degradation of phenol of TiO_2 and ZnO in the presence of manganese dioxides, Catal. Today. 139 (2008) 109–112.
[30] N. Barka, A. Assabbane, A. Nounah, Y. ÂıtIchou, Photocatalytic degradation of indigo carmine in aqueous solution by TiO_2-coated non-woven fibers, J. Hazard. Mater. 152 (2008) 1054–1059.
[31] A. Fujishima, T.N. Rao, D.A. Tryk, Titanium dioxide photocatalysis, J. Photochem. Photobiol. C: Photochem. Rev. 1 (2000) 1–21.
[32] R.T. Sapkal, S.S. Shinde, T.R. Waghmode, S.P. Govindwar, K.Y. Rajpure, C.H. Bhosale, Photo-corrosion inhibition and photoactivity enhancement with tailored zinc oxide thin films, J. Photochem. Photobiol. B: Biol. 110 (2012) 15–21.
[33] G. Kenanakis, Z. Giannakoudakis, D. Vernardou, C. Savvakis, N. Katsarakis, Photocatalytic degradation of stearic acid by ZnO thin films and nanostructures deposited by different chemical routes, Catal. Today 151 (2010) 34–38.
[34] V.V. Shvalagin, A.L. Stroyuk, S. Ya Kuchmii, Role of quantum-sized effects on the cathodic photocorrosion of ZnO nanoparticles in ethanol, Theoret. Exp. Chem. 40 (2004) 6.
[35] L. Zhang, H. Cheng, R. Zong, Y. Zhu, Photocorrosion suppression of ZnO nanoparticles via hybridization with graphite-like carbon and enhanced photocatalytic activity, J. Phys. Chem. C 113 (2009) 2368–2374.
[36] N.V. Kaneva, D.T. Dimitrov, C.D. Dushkin, Effect of nickel doping on the photocatalytic activity of ZnO thin films under UV and visible light, Appl. Surf. Sci. 257 (2011) 8113–8120.
[37] H. Zhang, R. Zong, Y. Zho, Photocorrossion inhibition and photoactivity enhancement for zinc oxide via hybridization with monolayer polyaniline, J. Phys. Chem. C 113 (2009) 4605–4611.
[38] A. Ranjbari, N. Mokhtarani, Kinetics study of UV-ZnO photocatalytic process for post treatment of composting leachate, Modares Civil Eng. J. (M. C.E.J.). 16 (2016) 123–133.
[39] E.S. Elmolla, M. Chaudhuri, Degradation of amoxicillin: ampicillin and cloxacillin antibiotics in aqueous solution by the UV/ZnO photocatalytic process, J. Hazard. Mater. 173 (2010) 445–449.